Seabed Characterization for SW2013 Mid-Frequency Reverberation Experiment

Charles W. Holland
The Pennsylvania State University
Applied Research Laboratory
P.O. Box 30, State College, PA 16804-0030
Phone: (814) 865-1724 Fax (814) 863-8783 email: holland-cw@psu.edu

Grant Number: N00014-12-1-0082

LONG TERM GOALS

The long-term science question addressed by the SW2013 experiment (relevant to this proposal) is to advance understanding of the seabed mechanisms that control clutter and diffuse reverberation

OBJECTIVES

The specific goals are to: 1) quantify seabed physical properties and their spatial (vertical and horizontal) variability and uncertainties and 2) based on the spatial variability make and test hypotheses about the mechanisms that control clutter and diffuse reverberation.

APPROACH

The observational approach is based on direct path measurements of seabed reflection. The key advantages of this approach are: high resolution (0.1 m vertically, 1-10 m laterally); relatively modest uncertainties (due to short path lengths) from the space/time varying oceanography and biology; and that low source levels are possible. The main challenge is that water depth, 20 m, is 4 times smaller than what has been achieved in the past which poses challenges for multipath separation and separation of angle dependence from lateral variability. The latter problem arises due to the small Fresnel zone size coupled with the shorter lateral variability scales that occur for inner shelf environments.

WORK COMPLETED

Two main tasks were completed in FY13: 1) planning and conduct of at-sea measurements in TREX'13 and 2) processing of the data to obtain the broadband spherical wave reflection coefficient.

RESULTS

At-sea measurements The at-sea measurements were conducted May 2013 from R/V Quest. Original plans called for a surface and sub-surface towed source. The main advantages of the surface towed source were to a) facilitate multipath separation, b) exploit long experience with conducting the experiments with the source and c) easily monitor source position. However, in the end it was possible only to use the sub-surface ITC-1007 source. An engineering trial, May 3, was successful in the first

deployment and retrieval of two Instruments Concepts (IC) self-contained receivers (which performed well), however, the source functioned only for 10 minutes. A second engineering trial was undertaken May 5 for several hours while R/V Sharp was in port due to bad weather. The source functioned properly during this trial, but high seas curtailed the trial. The main experiment was conducted on the morning of May 8 in very good weather, with three Loggerhead DSGmini receivers.

Data processing. An example of the data from May 8 is shown in Figure 1 – each vertical trace corresponds to a single ping received at the DSGmini hydrophone. The main paths in order of arrival are the: direct, bottom reflected, and sea surface reflected paths. The data processing exploits the direct path to measure the transducer beam pattern *in-situ*. Forming a ratio between the direct and bottom paths (accounting for spreading, attenuation and the source beam pattern) yields the seabed reflection coefficient (see Ref [1] for details on the processing and processing uncertainties). The faint arrivals immediately following the seabed reflected path are reflections from sub-bottom sediment structure which is of interest to the science goals.

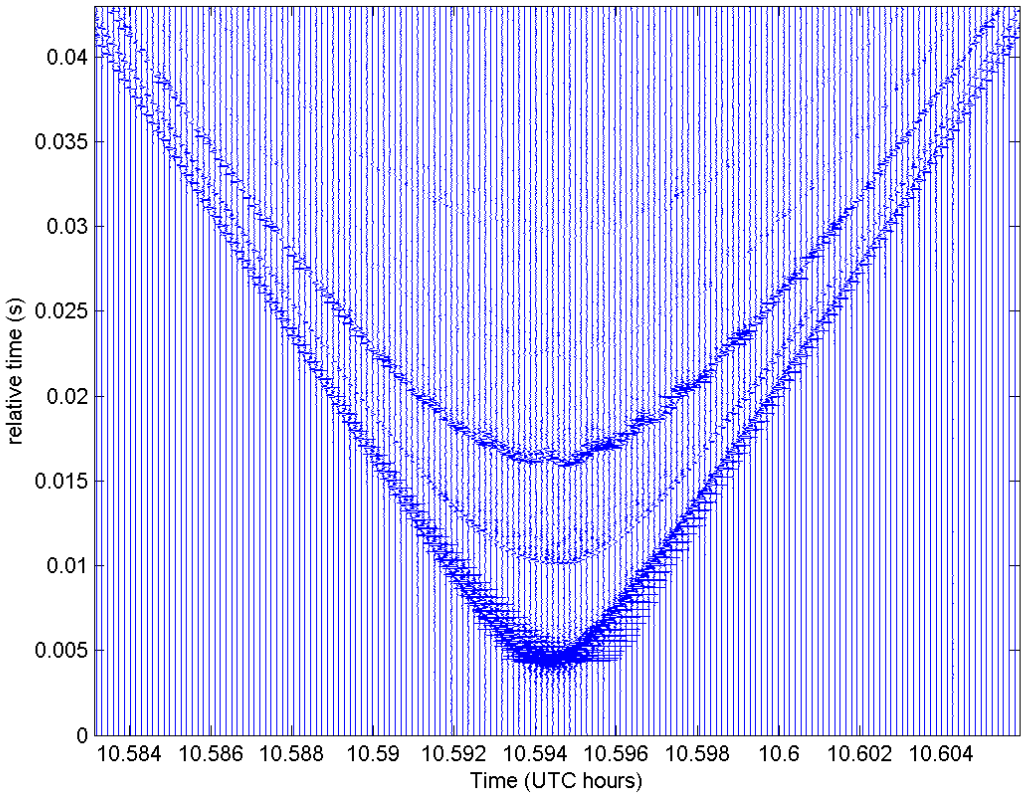

Figure 1 Matched filtered Doppler corrected time series (May 8) along the main reverberation line

The source transmitted a 12-1.4 kHz LFM down sweep equalized to the ITC-1007 transmit voltage response curve so that the signal in the water was nearly flat across the band at a 2 Hz repetition rate. While the source tow speed was just 3-4 knots and LFMs are often considered Doppler insensitive, the LFM length (250 ms) meant that Doppler effects were not negligible. An example is shown in Fig. 2, note for the source incoming towards the receiver, the matched filtered pulse without Doppler correction (blue) shows low to high frequency oscillations - on the outgoing portion of the source tow the high frequency oscillations are first. The match filtered pulse with the Doppler correction (in red) shows the correct pulse compression with a higher amplitude and narrower pulse than the uncorrected

pulse. The relative speed estimation is performed using a closed form solution developed by Samuel Pinson a post-doc working with the PI using the phase of the uncorrected arrival. This turned out to be a much better estimate than simply using the speed of the ship or that of the catamaran behind the ship (from whence the source was deployed). The importance of the Doppler correction is that it provides better multipath separation, i.e., better pulse compression.

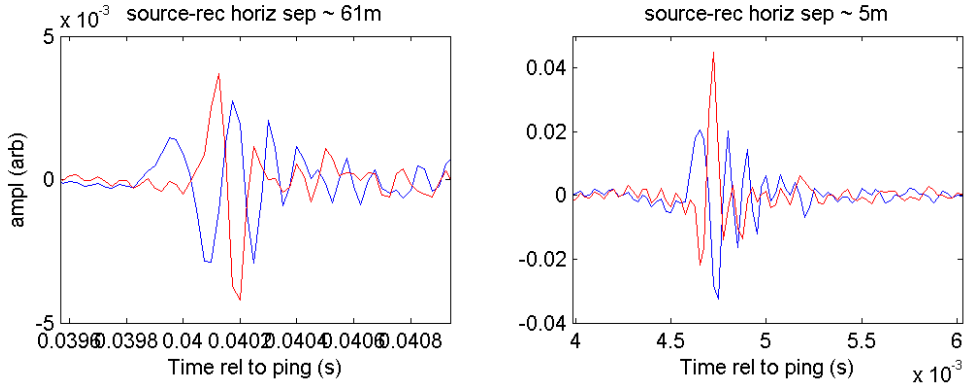

Figure 2 Comparison of the raw matched filtered arrival (blue) at 61 and 5 m horizontal offsets with the Doppler corrected matched filter pulse (red).

Figure 3 shows the direct path received level spectra for two receivers, the IC (left) and DSG (right) for the same source tow. The two receivers were within about 1 m apart. The main point of the plot is that the IC unit has a smooth behavior as a function of frequency and horizontal offset (which is related to vertical angle) whereas the DSG unit has a much more complicated behavior. Several explanations were proffered and explored, but the most likely explanation is scattering/multipath from the housing and brackets of the DSG unit. Modeling (using a finite-difference time domain solver Simsonic, [2]) indicated that this was the correct explanation since the modeling showed the same trends as the data. Further, the modeling was able to isolate the mounting bracket as a primary source of the scattered arrivals. Scattering from the epoxy filled contained with the batteries and a nearby self-recording temperature pod also contributed. Since modeling revealed that the scattered arrivals from above (direct path) were quite different from those below (seabed reflecting path), non-negligible uncertainties in the reflection coefficient could occur. Thus, at the present time, only data from IC units are considered for analysis.

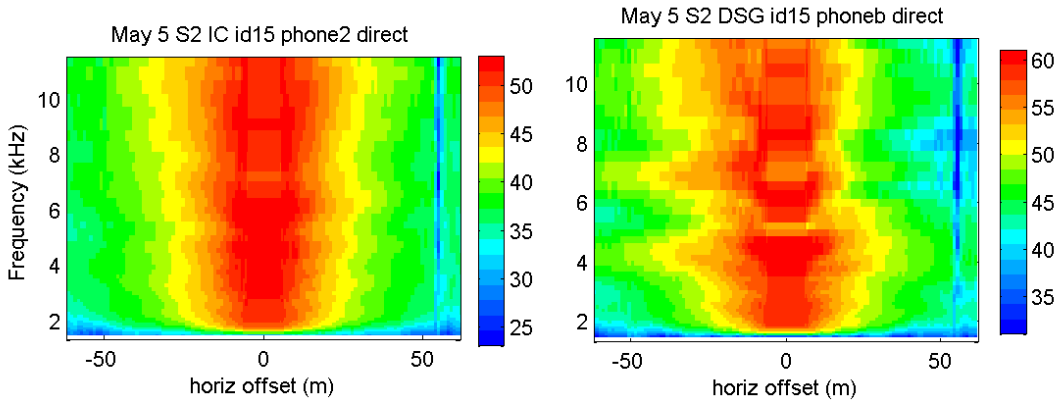

Figure 3 Comparison of direct path received levels on the IC unit (left) and DSG unit (right). The units are dB (arbitrary) and the scales have been adjusted to account for the difference in sensitivities between the two receivers. Note the complex DSG pattern suggesting multipaths/scattering.

In order to form the reflection coefficient, the geometry must be known. Since the clocks on the self-cording receivers are not sufficiently accurate to measure absolute time, the geometry (source-receiver separation) was estimated using relative arrival time differences between the direct, bottom , and surface. This algorithm was developed and implemented by Stan Dosso (UVic). The algorithm also estimated source and receiver depth, the former being poorly constrained in cases where the depth sensor above the source was not functioning.

Seabed wide angle reflection coefficient (vs angle and frequency)
With source levels vs angle (derived from the data in Figure 3, but not shown) and geometry known, the reflection coefficient **R** as a function of frequency and angle at the seabed can be computed. The results are shown in Figure 4 at two sites. Site 2 is along the main reverberation line roughly southeast 3.6 km from the reverberation source/receiver. The clutter site is roughly southwest 2.8 km of the reverberation source/receiver along the clutter track. The salient feature of the figure is the marked difference in **R**. At the clutter site there is a critical angle at ~28º, whereas it must be less than about 16º at Site 2. Assuming a homogeneous sediment halfspace this implies sediment sound speeds of ~1725 m/s and less than ~1585 m/s respectively.

While there is indubitably a substantial difference in seabed sound speeds between the two sites these estimates are very rough because 1) the measurements are spherical **R**, which exhibit critical angles somewhat less than the classical critical angle and 2) the homogeneous halfspace sediment approximation is likely poor. This is so because otherwise **R** would be nearly frequency independent. That there is structure/layering is seen in the coda following the seabed pulse in Figure 1 and also the classic striation patterns at Site 2 in Figure 4 (caused by quarter-wave resonances). The Clutter site also shows some evidence of layering, especially near the critical angle. In addition to layering, roughness and volume heterogeneities may also be present and play a role. There are a few regions of angle space at high frequencies that suggest that the seabed is not a plane-layered medium, nor can be described by statistical parameters (roughness or volume heterogeneities) at that frequency. For example, the peak in **R** at ~7.5 kHz and 38º at Site 2 suggests a seabed feature that is being mapped into angle but in reality is spatially localized. Analysis of the reflection data in terms of geoacoustic properties are in the early stages (with Jan Dettmer at UVic taking the lead using Bayesian methods).

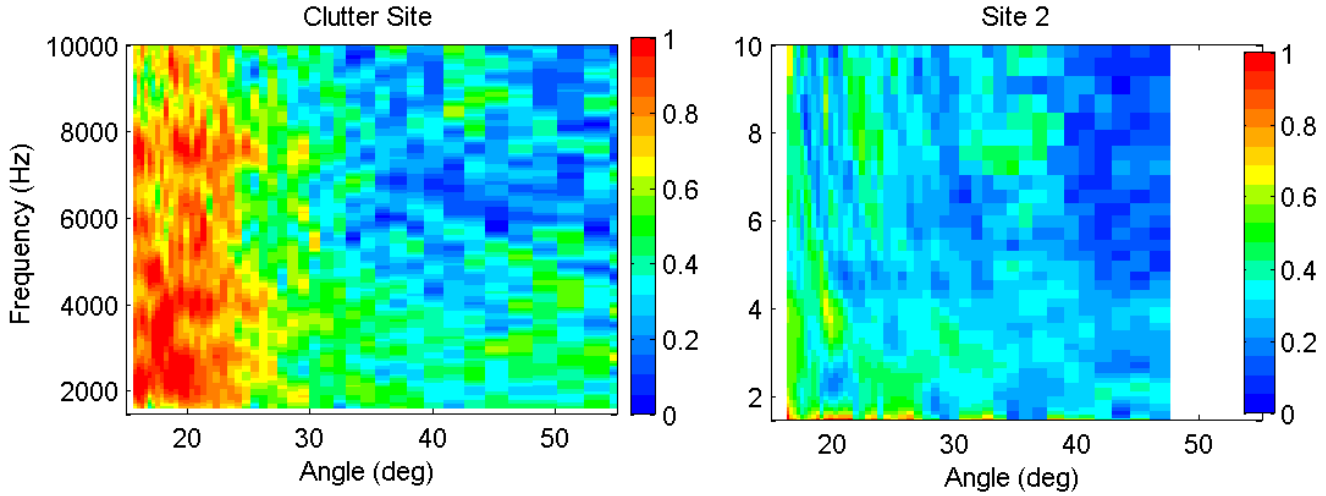

Figure 4 spherical pressure reflection coefficient at Clutter Site (May 3) and Site 2 May 5.

Seabed reflection coefficient at normal incidence

Normal incidence reflectivity was investigated (see Figure 5) close to the Site 2 wide angle reflection track. The normal incidence track (black), ~440 m in length, is superimposed on the 10 m bathymetry and (white) on the multibeam backscatter (from Chris DeMoustier and Barb Kraft) and goes from northwest to southeast. The wide angle reflection track is shown on the backscatter map (light green) going nearly west. The receiver for the wide angle measurements was nearly at the crossing point of the two lines. Part of the analysis motivation was to examine any laterally varying seabed structure that may be biasing into the angular dependence of the reflection coefficient (e.g., Figure 4 Site 2 at 38º). Note that the track begins and ends near two adjacent sand wave crests. The high frequency multibeam backscatter shows a smooth patch in the middle of the track with a north-south dark lineation running nearly through the intersection of the two tracks. Towards both ends of the track the backscatter shows a series of high backscatter lineations. It should be noted that there is some uncertainty (not quantified yet, but likely less than ~10 m) of absolute position accuracy in the track line data.

The magnitude of the peak broadband bottom reflection coefficient along the normal incidence track averaged over a lateral extend of ~6 m (5 pings) is shown in Figure 6. The source was the same as for the wide angle measurements but the receiver was a hydrophone approximately 2 m above the source on the same tow line. Note the strong drop in reflectivity at ~13.36 hr, where the change is almost a factor of 2 in amplitude. Both system (e.g., source depth or amplitude variation) and environmental factors to explain this drop have been explored. At present it seems unlikely that the observed variations are due to system effects.

For environmental effects, possible correlations with bathymetry (10 m lateral resolution) and/or high frequency backscatter were explored. Note that the overall bathymetry differences are very small, ~ 0.3 m (see bottom of Figure 6). Sediment wave crests near the beginning and end of the track may roughly correlate with the high reflection amplitudes, the low reflectivity with the deepest part of the track. However, the correlation is somewhat weak. Mechanisms causing the strong peaks at ~13.385 hr may occur from small scale sediment variability or from focusing caused by curvature in the boundary on the scale of the Fresnel zone, but are not understood at this time. A qualitative comparison of the wide angle and broadband normal incidence data shows that there are large spatial fluctuations in high normal incidence R close to the artifacts observed in the wide angle data (Figure 4 Site 2 at ~38º). This spatial correlation, suggests a linkage that needs to be explored.

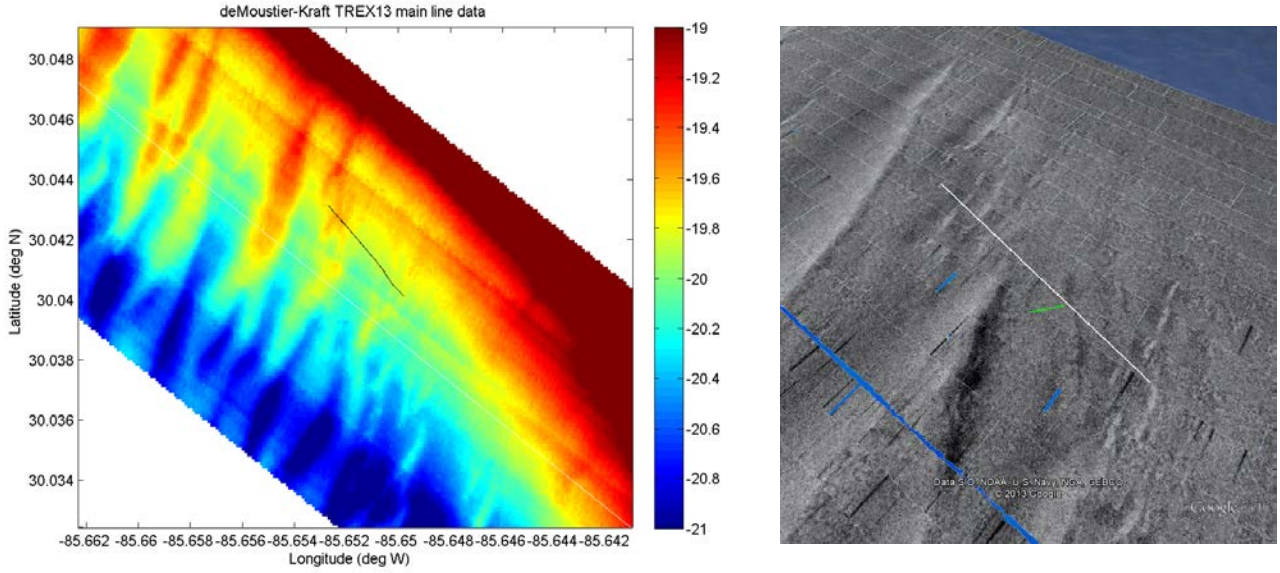

Figure 5. Bathymetry (left) with reflection line (black) and Reson multibeam backscatter map (right) with reflection line (white). The normal incidence track proceeds from northwest to southeast, the wide angle reflection (see data in Figure 4) track in light green is east to west, with the receive array at the eastern end. The backscatter data have a dynamic range of -18 dB (black) to -7 dB (white).

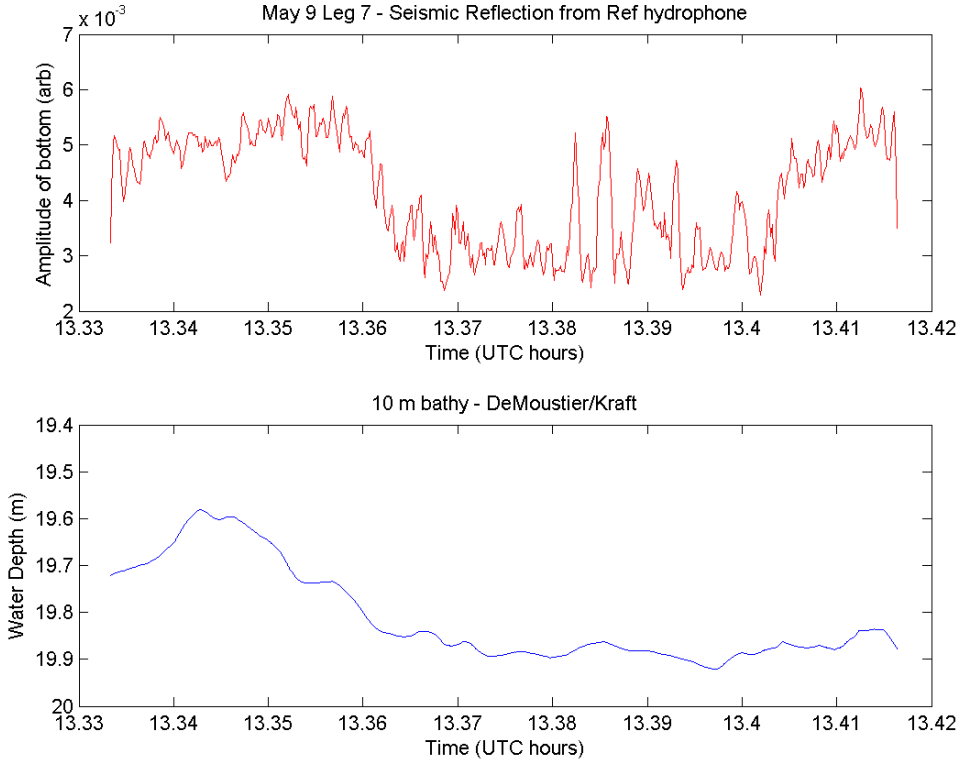

Figure 6. Normal incidence reflection coefficient along a track (see Figure 5) from northwest to southeast. The track nearly intersects with the wide angle reflection data of Figure 4 at ~13.39 UTC.

IMPACT/APPLICATIONS

The processed reflection data will be employed to estimate geoacoustic structure and uncertainties vs depth and frequency (we will incorporate dispersion in our inversions via a variant of Ref [3]). This will be important for 1) understanding the impact of sediment structure on propagation and reverberation and 2) may lead to identification of mechanisms that lead to clutter. A hypothesis posited before the experiment was that mud lenses can lead to clutter and/or high levels of reverberation. Mud lenses were discovered at the site, but their impact has not been explored yet. The derived geoacoustic model from the reflection data will assist in modeling the reverberation with as few unknown parameters as possible.

RELATED PROJECTS

ONR Seabed Geoacoustic Structure at the Meso-Scale: that project developed the machinery (forward models and inverse methods in collaboration with Jan Dettmer and Stan Dosso at UVic) for estimating geoacoustic properties and their frequency dependencies in complex layered media.

REFERENCES

[1] Holland C.W., Seabed reflection measurement uncertainty, J. Acoust. Soc. Am., 114, 1861-1873, 2003.

[2] Bossy, E., Padilla, F., Peyrin, F., and Laugier, P., Three-dimensional simulation of ultrasound propagation through trabecular bone structures measured by synchrotron microtomography," Phys. Med. Biol., 50, 5545–5556, 2005.

[3] Buckingham M.J., On pore-fluid viscosity and the wave properties of saturated granular materials including marine sediments, J. Acoust. Soc. Am. 122, 1486, 2007.